THE ASTROPHYSICAL JOURNAL, 391:518–530, 1992 June 1


# TIME SERIES ANALYSIS IN ASTRONOMY: AN APPLICATION TO QUASAR VARIABILITY STUDIES

R. VIO,[1] S. CRISTIANI,[1] O. LESSI,[2] AND A. PROVENZALE[3]
*Received 1991 July 8; accepted 1991 December 4*

## ABSTRACT

Many astrophysical objects can be associated with continuous non-linear stochastic systems. Up to now, however, the signals coming from these systems have been analyzed mainly through linear approaches, such as the power spectrum (PS) and the structure function (SF) techniques, frequently with controversial results.

In this paper we show that in the study of astronomical time series the PS (even in the maximum entropy or CLEAN version) and the SF techniques are often of little use or even misleading, since they do not take into account all the information contained in the data. New techniques, such as the bispectrum and multifractal analyses, are necessary to gain further insight into the dynamics of these systems. The effects of the discrete sampling of the signal are also considered, and the evolution of a single system and that of a multiple subunit system are distinguished. The approach based on phase-space reconstruction algorithms and on dimension and entropy estimators as derived from the theory of nonlinear dynamical systems is discussed as well.

In general, the need of developing more and more refined methods of statistical analysis is accompanied by the necessity of possessing an at least approximate a priori knowledge of the dynamics of the system under study.

*Subject heading:* methods: numerical — quasars: general

## 1. INTRODUCTION

The luminosity variations of astronomical objects are an important and widespread phenomenon which may provide considerable information on the dynamics of the system under study. In this paper we explicitly consider this topic and discuss the general problem of the analysis of temporal data in astronomy. This topic is examined in the context of quasar variability in order to test the performances of the various statistical methods in a given experimental ambit. Quasar studies have been chosen because they are representative of a remarkable situation: in spite of the large amount of available data (some objects have time series composed of hundreds of observations), in the last 20 years the variability studies have not provided major progress. In a recent paper (Vio et al. 1991), this fact has been explained with the fundamental nonlinearity of the quasar time series: quasars, being nonlinear physical systems whose temporal evolution is described by nonlinear dynamical equations, have light curves that cannot be analyzed only by means of the classical methods (e.g., PS, SF, and covariance analyses) which are suitable only for dealing the signals characteristic of linear systems. New statistical techniques are therefore required.

A second aim of this paper is to warn about the idea, which has become somewhat popular in recent years, that it is useful to develop methods of data analysis that do not take into account the physical origin of the signal. This idea is based on the assumption that by the sole knowledge of the signal it is possible to reconstruct the dynamics of the systems or even to derive the "equations of motion" that have generated it. Besides the tremendous technical difficulties, in the following we consider a few examples and we show that this approach can be misleading: dynamical information on the system under study turns out to be necessary.

[1] Dipartimento di Astronomia della Università di Padova, Vicolo dell' Osservatorio 5, I-35122 Padova, Italy.
[2] Dipartimento di Statistica della Università di Padova, Via S. Francesco 33, I-35122 Padova, Italy.
[3] Istituto di Cosmogeofisica del C.N.R., Corso Fiume 4, I-10133 Torino, Italy.

## 2. CLASSICAL TIME SERIES DATA ANALYSIS

In the astronomical literature, the "classical" tool for the analysis of temporal data is the PS analysis, which is useful for detecting the possible periodicities present in a signal (other techniques are, however, available; see, for example, Heck, Manfroid, & Mersch 1985; Nemec & Nemec 1985; Swingler 1989).

Many sophisticated algorithms for computing the PS of a time series are now available (see Marple 1987 for a review), but they are relatively seldom applied to astronomical problems. One reason is that these algorithms require equispaced data. Nevertheless the classical PS is preferred by the astronomers even when this condition is satisfied. The most serious problem of the classical PS is its noisiness, resulting in a "peaked" appearance, and, consequently, giving often the erroneous impression of some periodic components in the signal. An estimator of the PS that does not have this drawback is the so-called ME (maximum entropy) PS (Marple 1987; Ulrich & Bishop 1975), which is based on the principle of maximization of the entropy of the process. Besides the low noisiness, the ME PS has the property of a high sensitivity to the presence of periodic components in the signal. These properties hold also with time series formed by only 50–60 points.

In many astronomical situations, however, the available light curves have an irregular sampling. In this case the analysis of the PS is complicated by the presence of interference peaks (Deeming 1975; Scargle 1982; Horne & Baliunas 1986; Press & Rybicki 1989; Koen 1990) due to the convolution of the "true" discrete fourier transform (DFT) of the data

with the so-called spectral window (the DFT of the sampling time). Even more than before, the presence of a peak in a PS of a time series does not necessarily indicate the presence of a periodic component in the signal: a true periodicity in the data is characterized by a peak in the PS that increases continuously its intensity with time. Unfortunately, the interference peaks make difficult any analysis. Various methods developed for avoiding this problem have been suggested (Fahlman & Ulrych 1982; Sturrock & Shoub 1982; Scargle 1989; Brown & Christensen-Dalsgaard 1990). A very interesting approach has been proposed by Roberts, Lehar, & Dreher (1987). This method, a one-dimensional version of the well-known CLEAN algorithm, is based on the subtraction of the spectral window to the calculated DFT of the time series. Numerical simulations have shown that in the presence of an irregularly sampled periodic signal, the CLEAN algorithm is effectively able to recover most of the lost information. In Figure 1*a* we show as an example the PS of the light curve of the quasar 3C 446, obtained from the data reported by Barbieri et al. (1990). Figure 1*b* shows the same PS "deconvolved" with the CLEAN algorithm. Limiting the data to the first half of the available light curve, the "CLEANed" PS of Figure 1*c* has been obtained. Barbieri et al. (1990) stated that this object has a periodic component at about 1540 days. Notice how the peak corresponding to this periodicity increases its strength relatively to the other peaks for increasing times, supporting the original conclusion about the reality of this feature.

In recent years, the so-called structure function (SF) approach has become rather popular as well (Simonetti, Cordes, & Heeschen 1985). These functions represent a sort of "running" variance of the process, and their most useful feature is the ability to discern the range of time scales that contribute to the variations in a data set.

The PS and the SF techniques are, however, only a small subset of the statistical tools currently available, and, as it is shown below, they are not always appropriate to the physical problems under study. In the following we thus discuss the use of relatively "new" statistical techniques.

## 3. LINEAR AND NONLINEAR STOCHASTIC TIME SERIES ANALYSIS

An important finding about quasar variability has been the recognition of its unpredictable and irregular nature. Since 1968 Manwell & Simon realized that the time series of 3C 273 showed a "*noisy component*" which was not associated with measurement errors (see also Terrel & Olsen 1970). Since that time, this result has been confirmed by various authors for other objects (e.g., Moore et al. 1982; Lawrence et al. 1987; McHardy & Czerny 1987). This implies that the dynamical evolution of quasar luminosity cannot be described by periodic or quasi-periodic oscillations; in other words, quasars must be described by stochastic or chaotic dynamical systems. We now consider how quasar variability may be characterized in terms of stochastic processes. In particular, we stress the fact that, although the available quasar light curves are in form of discrete time series, the luminosity variations are continuous in time. Therefore, if we want to model the time evolution of the light emission, we have to use continuous models.

### 3.1. *Characterization of a Continuous Stochastic System*

The dynamical equations describing a physical, continuous, stochastic system can be generally written as (see the Appendix):

$$\dot{\boldsymbol{x}}(t) = \boldsymbol{f}[\boldsymbol{x}(t), \boldsymbol{u}(t), \boldsymbol{w}(t), t] \tag{1}$$

where $\boldsymbol{x}(t)$ is an $n$-by-1 state vector, $\boldsymbol{u}(t)$ is an $r$-dimensional input process, and $\boldsymbol{w}(t)$ is an $s$-dimensional white noise process. If the system is linear, equation (1) becomes:

$$\dot{\boldsymbol{x}}(t) = \boldsymbol{F}(t)\boldsymbol{x}(t) + \boldsymbol{B}(t)\boldsymbol{u}(t) + \boldsymbol{G}(t)\boldsymbol{w}(t)\,, \tag{2}$$

where $\boldsymbol{F}(t)$ is the $n$-by-$n$ *state* matrix, $\boldsymbol{B}(t)$ is the $n$-by-$r$ *input*

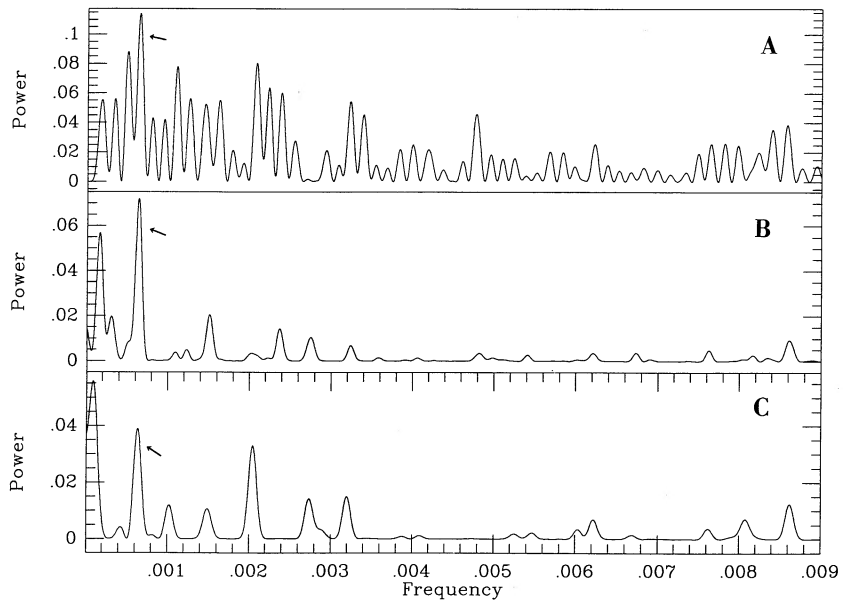


FIG. 1.—(*a*) Power spectrum of the complete light curve of 3C 446; (*b*) PS of the same data but with the CLEAN algorithm; (*c*) same as in (*b*) but limited to the first 6000 days. The abscissae are in units of day$^{-1}$. Notice the increase of intensity relative to the noise, from (*c*) to (*b*), of the peak (indicated by the arrow) corresponding to a periodicity of 1540$^{d}$.

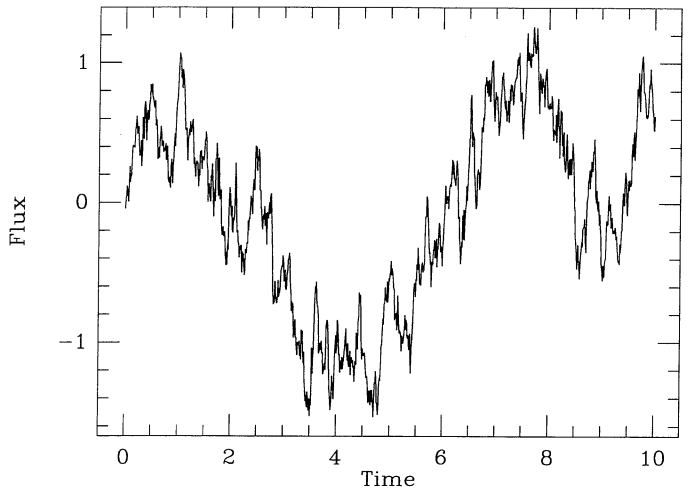


FIG. 2a

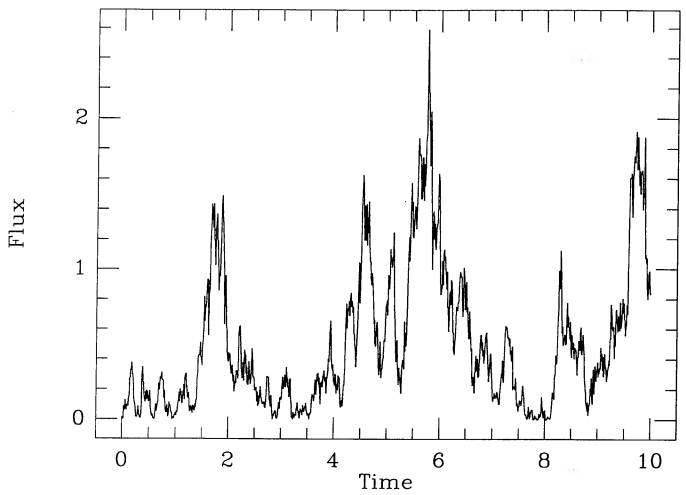


FIG. 2b

FIG. 2.—(*a*) Time series generated by the linear model (3) ($\theta = -0.9$, $\sigma = 1.0$, $\Delta t = 0.01$, 1000 points); (*b*) time series generated by the nonlinear model (4) ($\alpha = 1.0$, $\beta = 1.0$). Note the similarity of this signal with the light curves of OVV quasars such as 3C 446 (Barbieri et al. 1990) or 3C 345 (Vio et al. 1991).

matrix, and $\boldsymbol{G}(t)$ is the $n$-by-$s$ *noise* matrix. A useful characteristic of these systems is that they can be solved "exactly" (see the Appendix).

In case of a stationary scalar process with no input $u(t)$, equation (2) can be written as

$$\dot{x}(t) = \theta x(t) + \sigma w(t) \,. \tag{3}$$

Figure 2*a* shows a time series generated by the process (3) with $\theta = -0.9$,[4] $\sigma = 1$, and $w(t)$ as a standard Gaussian white noise process.

In a recent paper, Vio et al. (1991) have shown that the light curve of the OVV 3C 345 cannot be reproduced by means of linear processes. If the physical system is nonlinear, the situation becomes complicated because in general it is not possible to solve equation (1) exactly (see the Appendix).

Figure 2*b* shows a realization of the nonlinear process:

$$\dot{x}(t) = (\alpha - 0.5)\beta - x(t) + \sqrt{2\beta x(t)}\, w(t) \tag{4}$$

with $\alpha = 1.0$, $\beta = 1.0$, and $w(t)$ as a standard Gaussian white noise process. A comparison of Figure 2*a* with Figure 2*b* clearly shows that the two time series are different, the nonlinear one being characterized by the presence of positive "bursts" of enhanced activity. The Keenan test (Keenan 1985) confirms that the time series of Figure 2*b* is nonlinear (95% confidence). However, the (maximum entropy) power spectra of the two signals are very similar (see Fig. 3). This fact demonstrates that the PS is not able to use all the information contained in the data. The reason is that this technique uses only the first two moments of the process. The use of a PS method is sufficient if the system is linear and the $w(t)$ process is Gaussian, since the probability distribution function of the signal $x(t)$ is Gaussian too (only the Gaussian distribution can be completely described by the first two moments). But if the system is nonlinear, the probability distribution function of the $x(t)$ is not Gaussian any longer; the knowledge of moments of order higher than 2 is required. A similar situation holds for the SF technique; Figure 4 shows the SF of the two time series: again, it is impossible to distinguish the two processes.

[4] The parameter $\theta$ must be negative in order to avoid the "explosion" of the time series.

### 3.2. *Bispectrum and Other Statistical Methods*

A technique based on the principle of using the higher moments of the processes is the *bispectrum analysis.* The bispectrum of a discrete time series $x_0, x_1, \ldots, x_{N-1}$ is defined as

$$\hat{B}(\omega_1, \omega_2) = \sum_{k_1=-(N-1)}^{(N-1)} \sum_{k_2=-(N-1)}^{(N-1)} \hat{r}(k_1, k_2) W(k_1, k_2) \times \exp\left[-i(\omega_1 k_1 + \omega_2 k_2)\right] ,$$

where

$$\hat{r}(k_1, k_2) = \frac{1}{N} \sum_{t=0}^{N-\gamma} (x_t - \bar{x})(x_{t+k_1} - \bar{x})(x_{t+k_2} - \bar{x}) \qquad (\gamma = \max\,[0, k_1, k_2])$$

is the sampled three-point autocovariance function of the time series, and $W(k_1, k_2)$ is a two-dimensional window function used with a smoothing purpose (Subba Rao & Gabr 1984;

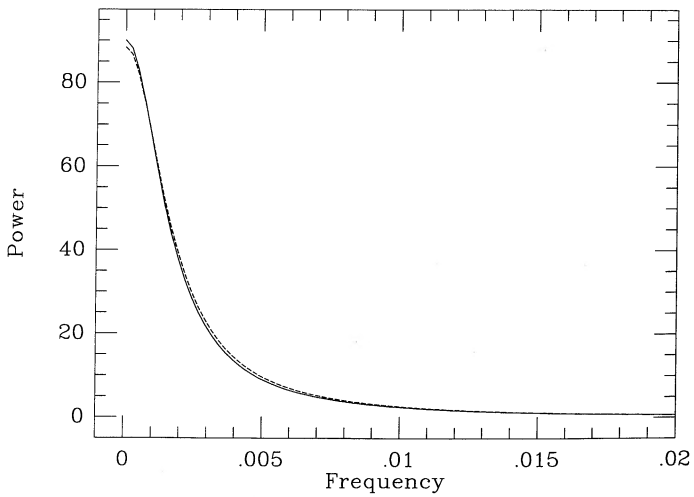


FIG. 3.—ME power spectra of the time series shown in Fig. 2*a* (*continuous line*) and Fig. 2*b* (*dashed line*) [abscissae in units of $(\Delta t)^{-1}$].

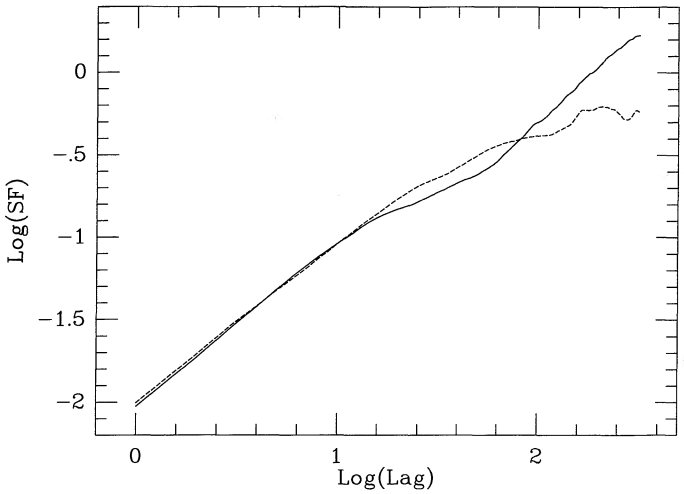


FIG. 4.—First-order structure functions of the time series shown in Fig. 2*a* (*continuous line*) and in Fig. 2*b* (*dashed line*), in logarithmic coordinates.

Chrysostomos & Mysore 1987). Using the three-point autocovariance function, the bispectrum exploits up to the third moment of the processes; therefore, with nonlinear time series it is more powerful than the classical power spectrum. Unfortunately the bispectrum has two serious drawbacks (Chrysostomos & Mysore 1987):

1. In absence of any "a priori" information, the results that it provides are of difficult interpretation.
2. It is a very noisy function.

Besides these well-known points, from numerical simulations it appears that the truncation and aliasing effects are more serious than for the classical Fourier transform, and sometimes they can unacceptably alter the results. Figures 5*a* and 5*b* show the modulus of the (unfiltered) bispectra for the time series in Figures 2*a* and 2*b*. Note that, although in principle the modulus of the bispectrum of a linear Gaussian process should be equal to zero, Figure 5*a* shows a peak near the origin. This effect is explained considering that the bispectrum of a linear (not necessarily Gaussian) process is given by (Subba Rao & Gabr 1984):

$$B(\omega_1, \omega_2) = \frac{\mu_3}{(2\pi)^2} H(\omega_1)H(\omega_2)H^*(\omega_1 + \omega_2) ,$$

where $\mu_3$ is the third moment of the white noise process $w(t)$, and $H(\omega)$ is the DFT of the process. For a Gaussian process, $\mu_3$ should be equal to zero and therefore it should be $B(\omega_1, \omega_2) = 0$ for every frequency. However, since in practice $\mu_3$ can only be estimated ($\hat{\mu}_3$ will never be exactly equal to zero), and since the modulus of the DFT of the considered process is a strongly decreasing function of $\omega$, the modulus of the quantity $\hat{\mu}_3 \hat{H}(\omega_1)\hat{H}(\omega_2)\hat{H}^*(\omega_1 + \omega_2)$ will quickly increase for frequencies $\omega_1$ and $\omega_2$ approaching zero. This means that great care has to be adopted in analyzing the bispectrum of a (positively autocorrelated) signal near the frequency origin. In any case, the difference between Figures 5*a* and 5*b* is clearly visible, indicating that the bispectrum is able to recognize the different nature of the time series. From a physical point of view, this difference is due to a phase coupling at some frequencies (NB: contrary to the PS, the bispectrum takes in account the phase information). A possible way of showing that the phase coupling plays a crucial role is based on substituting the actual DFT phases of the nonlinear signal with independent, randomly distributed uniform phases (a distribution which is typical of the linear stochastic signals). If the properties of the nonlinear signal are due to phase couplings, then they must be destroyed by this procedure. In fact, the time series obtained by inverting the DFT of the signal in Figure 2*b* with the phases uniformly randomized in the interval $0–2\pi$ shows characteristics similar to those of the linear process in Figure 2*a* [i.e., a Gaussian distribution of $x(t)$, the absence of positive "bursts" in the signal, the negative response of the Keenan test]. It is interesting to note that the phase coupling in the nonlinear process shown in Figure 2*b* concerns only a few frequencies since a Kolmogorov-Smirnov test is unable to discriminate the nonuniformity of the phase distribution. The bispectrum provides the relevant information on the coupled frequencies. In Figure 6 we show as an example the bispectrum modulus of the rebinned (800 bins) light curve of the OVV quasar 3C 345; its shape indicates a strong phase coupling (and therefore a definite nonlinearity of the process) among the frequencies in the range 0–0.1 (in units of $\sim 0.1$ day$^{-1}$). However, the physical interpretation of this result is still elusive.

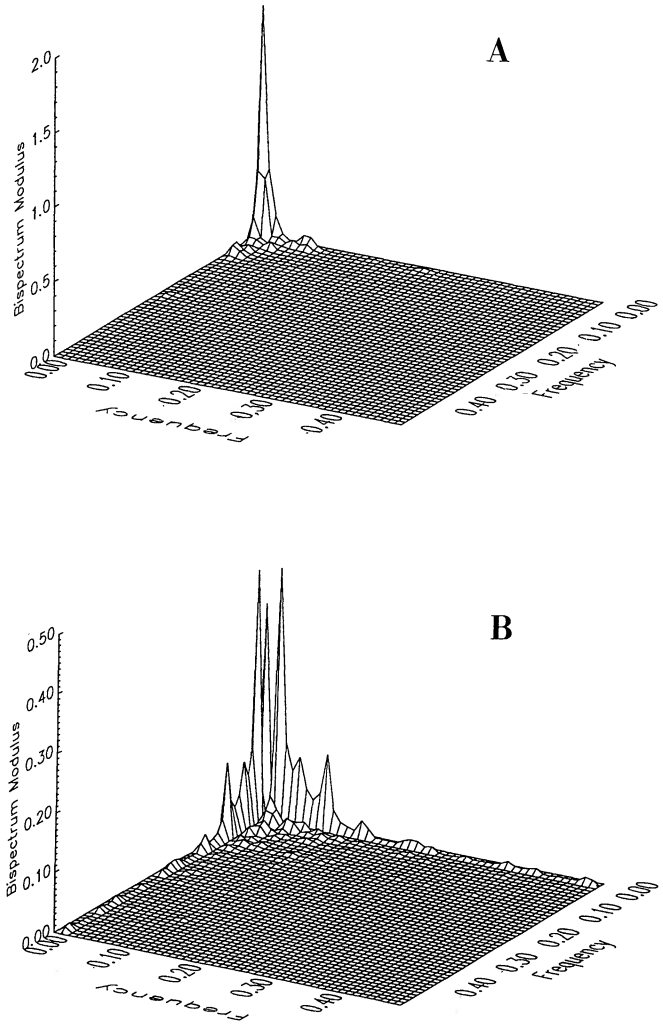


FIG. 5.—Moduli of the (unwindowed) bispectra of the time series shown in Figs. 2*a* and 2*b*, respectively. Frequencies in units of $(\Delta t)^{-1}$.

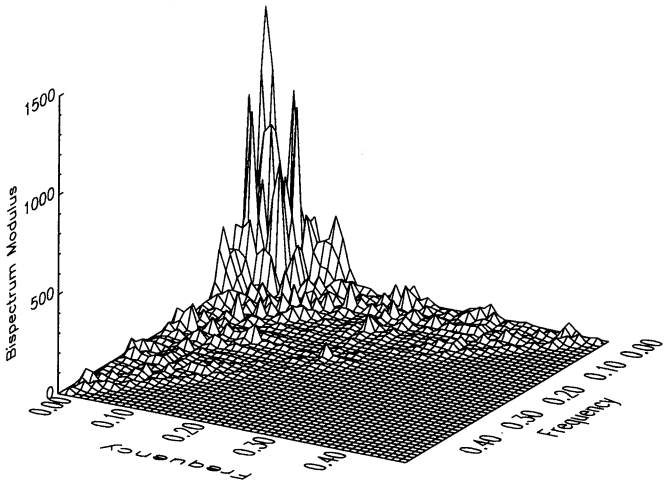


FIG. 6.—Modulus of the (unwindowed) bispectrum of the 3C 345 light curve. Frequencies in units of $\sim 0.1$ day$^{-1}$.

In the field of nonlinear, *discrete* time series analysis, a promising technique is represented by the so-called SDM (state-dependent models) (Priestley 1980, 1988). The interesting properties of this general class of models is that they are able to identify, at least in principle, the specific kind of nonlinearity present in the data without any "a priori" information. The SDMs have allowed to establish that the OVV quasar 3C 345 is a nonlinear stochastic system in a state of unstable equilibrium (Vio et al. 1991). In spite of their remarkable theoretical properties, the use of the SDM, even in the discrete case, is still limited to the identification of only a restricted number of nonlinear models (see Vio et al. 1991). Therefore, in the continuous case the SDM appears, at the moment, of limited use. For example they are not able to recognize that the time series of Figure 2*b* is nonlinear.

In the literature other nonlinear, discrete, stochastic models are available: bilinear (Subba Rao & Gabr 1984), threshold autoregressive (Tong 1983), and exponential autoregressive (Ozaki 1985). In general, however, the utility of these discrete models is limited, since they have been developed only with forecasting purposes.

### 3.3. *Sampling Time Effects*

The influence of the data sampling time on the results of the analysis has often been neglected. However, if the continuous nature of the signal is not explicitly taken into account, the results provided by any method of analysis are in general to be expected to depend on the sampling time.

To quantify this point, we reconsider the linear process (3). As shown in the Appendix, the evolution of such a process can be represented by means of a difference equation:

$$x_{t+1} = \alpha x_t + e_{t+1} , \tag{5}$$

where $e_{t+1}$ is a discrete white noise process. From the point of view of classical time series analysis, such a system represents an AR(1) model. This fact could suggest the possibility of obtaining information on a linear physical system by fitting the signal with the classical stochastic discrete models such as AR (autoregressive), MA (moving average), and ARMA (autoregressive moving average) (see Scargle 1981). Unfortunately, this is not true since the values of $\alpha$ provided by discrete algorithms critically depend on the sampling frequency. For example, using the results of the Appendix, it is possible to see that the parameter $\alpha$ of the discrete process (5) is linked with the parameter $\theta$ of the corresponding continuous process (3) by

$$\alpha = \exp(\theta \Delta t) , \tag{6}$$

where $\Delta t$ is the sampling time. Therefore, if the sampling frequency decreases (recall that $\theta$ must be negative), the value of $\alpha$ goes to zero. In other words, if a signal is observed at discrete instants, it will tend to appear as white noise for $\Delta t \to \infty$. This happens because the covariance between the values of consecutive instants, a measure of the signal coherence, scales as $\exp(\theta \Delta t)$.

The situation becomes even more critical with systems of order greater than one. In fact, the dynamical system:

$$\ddot{x}(t) + \theta_1 \dot{x}(t) + \theta_0 x(t) = w(t)$$

can be easily shown to be equivalent to a discrete ARMA(2,1) model (see for example Pandit & Wu 1975):

$$x_t - \phi_1 x_{t-1} - \phi_2 x_{t-2} = e_t - \psi e_{t-1} , \tag{7}$$

where

$$\phi_1 = \exp(\mu_1 \Delta t) + \exp(\mu_2 \Delta t)$$

$$\phi_2 = \exp[(\mu_1 + \mu_2)\Delta t]$$

$$\psi = \frac{(\mu_1 - \mu_2)[\mu_2 e^{\mu_2 \Delta t} - \mu_1 e^{\mu_1 \Delta t} + e^{(\mu_1 + \mu_2)\Delta t}(\mu_2 e^{\mu_1 \Delta t} - \mu_1 e^{\mu_2 \Delta t})]}{(\mu_2 e^{\mu_1 \Delta t} - \mu_1 e^{\mu_2 \Delta t})^2 + \mu_1 \mu_2 (e^{\mu_1 \Delta t} - e^{\mu_2 \Delta t})^2 - (\mu_1 - \mu_2)^2}$$

$$\mu_1, \mu_2 = \frac{-\theta_1 \pm \sqrt{\theta_1^2 - 4\theta_0}}{2} .$$

Apart from the already mentioned "whiteness appearance" of the signal for $\Delta t \to \infty$, it is important to note that, at variance with the classical ARMA(2,1) models, the model (7) has only two independent parameters: once $\mu_1$ and $\mu_2$ are known, the three parameters $\phi_1$, $\phi_2$, and $\psi$ are completely determined. These facts imply that the parameters of the model (7) cannot be estimated by means of the classical ARMA algorithms, since they assume the independence of the characteristic parameters.

In the nonlinear case, the effects of the sampling time cannot be modeled in a simple way, since it is difficult to construct equivalent discrete representations of the continuous processes. In general, however, some conspicuous consequences are to be expected, especially in regard to the possibility of recovering the kind of nonlinearity of the process. For example, if the characteristic time of the sampling is doubled, both the Keenan test and the bispectrum are not able to realize the nonlinearity of the time series of Figure 2*b*. This last point has important implications.

Statistically, a given process could display certain kind of nonlinearities or even appear as a linear process, depending only on the frequency sampling.

### 3.4. *Techniques of Multifractal Analysis*

Besides the statistical methods described in the previous sections, other approaches to the characterization of experimental signals come from methodologies developed in the context of nonlinear physics.

In general the signal generated by a linear and Gaussian stochastic process has a Gaussian distribution of the increments $\Delta x(t) = x(t + \Delta t) - x(t)$. On the contrary, the distribution of increments for a nonlinear signal often shows the

existence of quasi-exponential tails of the kind $P(\Delta x) \approx \exp(-\alpha \Delta x)$, as reported in Figure 7 for the signal of Figure 2*b*. Exponential tails may be a sign of the so-called *intermittency* phenomenon (see, e.g., Paladin & Vulpiani 1987 and quoted references therein), i.e., of the fact that the signal can display occasional strong bursts of enhanced activity interwoven with long periods of "quiet" activity. In fact, exponential tails imply a probability of large increments which is much larger than Gaussian. The time series of velocity and of velocity gradients in turbulent flows are a classic example of intermittent signals, see, e.g., Basdevant et al. (1981), Benzi et al. (1984, 1986), Frisch & Parisi (1985), Paladin & Vulpiani (1987), and Sreenivasan & Meneveau (1988).

A quantitative way of characterizing the intermittent behavior is the determination of the *multifractal properties* of the signal under study. Fractal objects are now widely used in the modeling and interpretation of natural phenomena (see, e.g., Mandelbrot 1982; Pietronero & Tosatti 1986; Schertzer & Lovejoy 1987; Martinez et al. 1990; Heck 1990; Heck & Perdang 1991), due to their capability of compacting the information on the scaling and clustering behavior of the system. In this paper, we do not consider the dynamical implications of fractality, but we use the multifractal analysis methods as a *tool* for extracting information from a given signal, analogous to what is done by the PS analysis or by other statistical methods. Since intermittency is associated with multifractality, the detection of a multifractal behavior is an indication of the presence of intermittency in the data set under study.

A basic ingredient in the study of fractal sets is the definition of the fractal (or box-counting) dimension. To be consistent with the analysis of time series, here we consider the case of a set of points on a line (such as the set of measured data points as a function of time); the extension to larger ambient spaces is trivial. In general, one is interested in appropriately measuring the portion of the time axis which is occupied by the parts of the signal with "enhanced activity." For example, if we consider the time series of the squared increments $(\Delta x)^2$, which may be taken as a positive-defined measure of the power of the fluctuations in the signal (i.e., of the "activity" of the system; Sreenivasan & Meneveau 1988), we could take only those parts of the time series characterized by $(\Delta x)^2$ greater than a given threshold $\Delta_0^2$, and measure the portion of the time axis occupied at varying $\Delta_0^2$. The appropriate characterization of this quantity is provided by the "fractal dimension" of the distribution of the data points with $(\Delta x)^2 \geq \Delta_0^2$. The fractal dimension $D^{(0)}$ of a point set on a line (say the time axis) is given by

$$D^{(0)} = \lim_{\epsilon \to 0} \frac{\log N(\epsilon)}{\log 1/\epsilon},$$

where $N(\epsilon)$ is the number of segments with duration $\epsilon$ which are needed to cover completely the point set. If $D^{(0)}$ is equal to one, then the point set under study covers completely the line; in this case the point distribution may be considered to be essentially homogeneous. If $D^{(0)} < 1$, then the points do not cover completely the line, in this case a hierarchy of dishomogeneities exist in the distribution.

The definition of the box-counting dimension can be generalized for calculating the entire spectrum of the generalized fractal dimensions. This can be done by associating a measure $\mu_i(\epsilon)$ to each one of the $N(\epsilon)$ segments with size $\epsilon$ which are used in the covering procedure. In the simplest case, this measure may be the number of points covered by each segment; more generally, the measure $\mu_i(\epsilon)$ of the $i$th segment is provided by the sum of the "strengths" associated with the points covered by the segment, i.e., by the integral of the square of the time series over the $i$th segment. The generalized dimensions $D^{(q)}$ are then defined as

$$D^{(q)} = \frac{1}{q-1} \lim_{\epsilon \to 0} \frac{\log \sum_{i=1}^{N(\epsilon)} [\mu_i(\epsilon)]^q}{\log \epsilon}.$$

The generalized dimensions $D^{(q)}$ at increasing $q$'s refer to the distribution of the higher moments of the signal. Thus, computing the generalized dimension for increasing values of $q$ is essentially equivalent to computing $D^{(0)}$ for increasing values of $\Delta_0^2$. However, the calculation of the generalized dimensions $D^{(q)}$ is in general more stable and it must be preferred. If all the generalized dimensions are equal, then the signal is monofractal and no intermittency is present; on the contrary, in the general case $D^{(q)} > D^{(q')}$ for $q < q'$ the signal is multifractal and intermittent (Benzi et al. 1984; Halsey et al. 1986; Paladin & Vulpiani 1987). In other words, an intermittent signal is characterized by the fact that its higher moments are less and less "line filling" (i.e., they are more rare) as the order of the moment increases.

Before applying the multifractal analysis to a given stochastic signal, we have first to select an appropriate measure. Clearly, the measure must be positive-definite. A good measure for a time series may be obtained by considering the integral of the square of the increments of the signal on each of the $N(\epsilon)$ segments, i.e.,

$$\mu_i(\epsilon) = \sum_{j=1}^{M} [\Delta x(t_j)]^2 \Theta[t_j - (t_i - \epsilon/2)] \Theta[(t_i + \epsilon/2) - t_j] \Delta t,$$

where $\Theta(t)$ is the Heaviside step function, $M$ is the total number of points in the time series, and, $t_i - \epsilon/2$ and $t_i + \epsilon/2$ are, respectively, the lower and upper edges of the $i$th segment with duration $\epsilon$ centered in the point $t_i$.

Figure 8 reports the results of the multifractal analysis for the linear signal in Fig. 2*a* and for the nonlinear one in Fig. 2*b*. For simplicity, the generalized dimensions have been computed only for $q$ varying from $q = 0$ to $q = 4$, due to the limited number of points in the time series. In this way, the results indicate exactly the type of behavior which could be encoun-

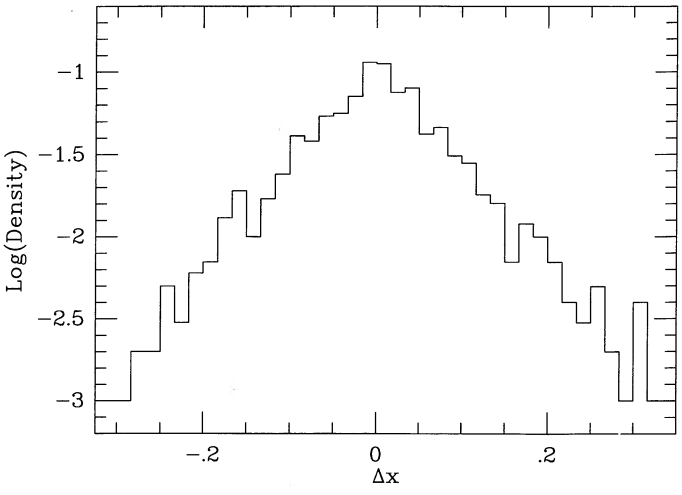


FIG. 7.—Logarithm of the distribution of the increments $\Delta x(t)$ for the nonlinear time series shown in Fig. 2*b*.

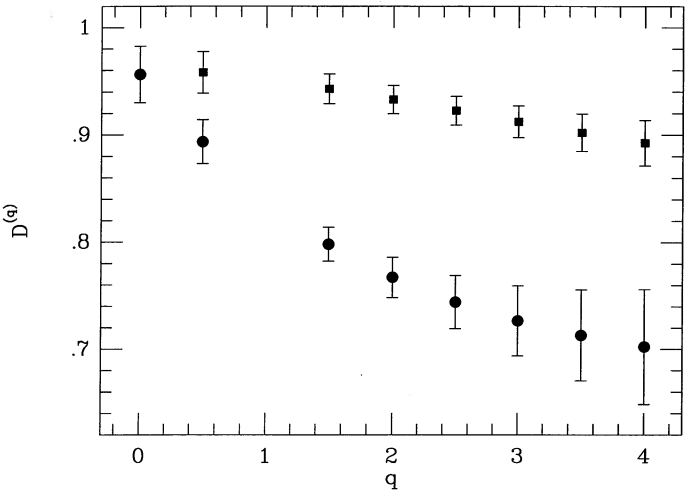


FIG. 8.— Generalized dimensions $D^{(q)}$ vs. $q$ for the linear time series (*filled squares*) and for the nonlinear one (*filled circles*) shown in Figs. 2*a* and 2*b*, respectively. The error bars are the 95% confidence limits on the linear least-squares fit of log ($Z$) vs. log ($\epsilon$) in the scaling range.

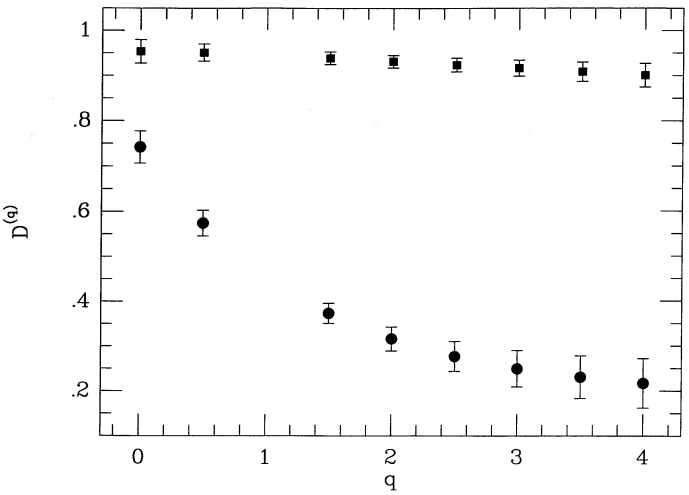


FIG. 9.—Generalized dimensions $D^{(q)}$ vs. $q$ for the light curves of PKS 2155−304 (*filled squares*) and of 3C 345 (*filled circles*). The error bars are the 95% confidence limits on the linear least-square fit of log ($Z$) vs. log ($\epsilon$) in the scaling range.

tered in the analysis of real quasar time series. Note also that the finite number of data points does not allow for taking the limit $\epsilon \to 0$ in the definition of the generalized dimensions. This situation is common to all analyses of experimental or numerical data; the common approach is to verify the scaling behavior of the partition functions $Z(\epsilon, q) = \sum_{i=1}^{N(\epsilon)} [\mu_i(\epsilon)]^q$ (i.e., their power-law dependence on $\epsilon$), and then to compute the generalized dimensions from the linear least-square fit of log $Z$ versus log $\epsilon$ in the scaling range.

The $D^{(0)}$ dimension is about one for both the signals considered here, indicating that the signals themselves are line-filling. For higher values of $q$, a decrease of the generalized dimension with increasing order $q$ is observed for both the linear and the nonlinear time series. However, in the case of the linear signal the decrease of the dimension is quite limited, and it may be entirely ascribed, as numerical simulations have shown, to a lack of statistics in the time series (higher order moments are more sensitive to the problem of a limited number of data points). Thus, the linear signal is monofractal and nonintermittent. On the other hand, the situation is completely different for the nonlinear signal. In this case, the decrease in the generalized fractal dimension with increasing $q$ is quite strong and cannot be ascribed to the limited statistics. For the nonlinear signal, the higher moments are *not* line filling; the signal is thus intermittent.

In Figure 9 we show, as an example, the generalized dimensions $D^{(q)}$ for $0 \leq q \leq 4$ for the X-ray light curve of the BL Lac object PKS 2155−304 (Tagliaferri et al. 1989) and for the optical light curve of quasar 3C 345 (Vio et al. 1991). While the X-ray curve displays a continuous "white noise" activity superposed to a long-term trend, the light curve of 3C 345 displays isolated periods of strong activity in a generally quiescent background. From Figure 9 one sees that the X-ray curve does not show any multifractality, the dimension decreasing from a value of about 0.95 for $q = 0$ to a value of about 0.9 for $q = 4$, consistent with the results found in the case of linear monofractal signals. By contrast, the light curve of 3C 345, in accordance with the previous analyses based on the SDMs, shows a clear evidence of a strong multifractal and nonlinear behavior. Note that for this signal $D^{(0)}$ is about 0.75; since the light curve of 3C 345 is irregularly sampled, this indicates that the signal itself is not line filling due to lack of data points in the time series. However, the strong decrease of the dimensions $D^{(q)}$ for $q > 0$ clearly indicate the multifractal and nonlinear nature of this process.

### 3.5. *Some Trends in the Analysis of Stochastic Dynamical Systems*

The methods presented above provide only a statistical characterization of the signals under study. As seen in the previous sections, several ambiguities are encountered when attempting to reconstruct the system dynamics from the analysis of a single time series. In order to recover the dynamics of a continuous system, it is therefore necessary to know (at least approximately) the kind of processes governing its evolution.

A possible way of obtaining the stochastic equations describing the dynamics of a given physical system is to dirty its characteristic equations. In the case of quasars, this operation could be carried out on the characteristic equations of the various models for the "fueling machine." Afterward, one could try to fit the "dirtied" equations to the observed time series. For example, in the case of the time series in Figure 2*a* it is possible to calculate analytically an estimate for the parameter $\theta$ of the model (3), throughout equations (5) and (6), by means of a least-squares algorithm (in this case, exactly equivalent to the maximum likelihood one) given that the sum of the squared residuals is

$$S^2 = \sum_t (x_{t+1} - x_t e^{\theta \Delta t})^2 .$$

The result obtained is

$$\hat{\theta} \simeq -0.96 .$$

Unfortunately, this good result has been obtained "almost by chance" since, as Figure 10 shows, the estimator of the $\theta$ parameter has a very dispersed distribution. This indicates, especially if one keeps in mind that the process simulated in Figure 2*a* is not a very noisy one, that in general the fitting of stochastic equations to an observed time series is not a

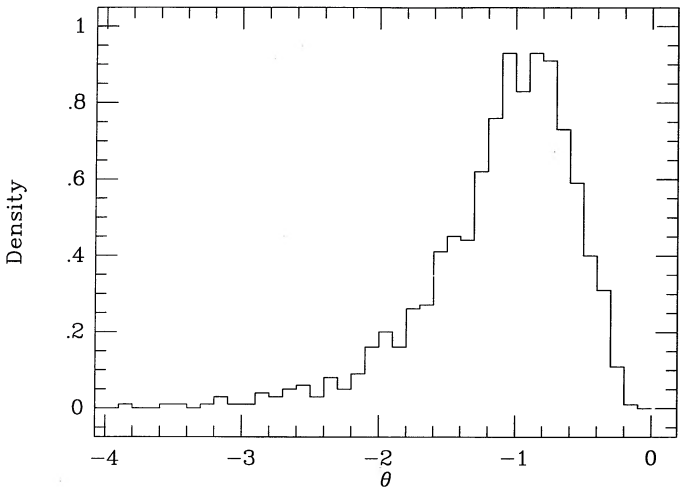


FIG. 10.—Distribution of the $\theta$ parameter obtained from the least-squares estimator for the linear model (3). The parameter values are the same used for the time series shown in Fig. 2*a*; a total of 1000 simulations have been considered.

straightforward operation. The situation becomes even more unfavorable with systems of order greater than one and/or with nonlinear systems. Moreover, there is the problem of the measurements errors that "dirty" the data with a noise which is not intrinsic to the system. Some algorithms are able to deal with this situation (see, e.g., Segal & Weistein 1987 for a review), but their use is very complicated, and their performances, except in very simple cases, are not known (this is the reason why statisticians have elaborated the discrete models).

At the moment, in our opinion, a more satisfactory approach is to assume some values for the parameters of the dirtied dynamical equations, to solve these with the methods of the local linearization, or of the numerical approximation, as indicated in the Appendix, and to compare, on the basis of their bispectra, multifractal properties and probability distributions, the synthetic curves obtained from the models with the observed ones. In this way it becomes available the "a priori" information necessary to interpret the results provided by the data analysis methods.

## 4. CHAOTIC ANALYSIS

The irregular and unpredictable behavior of a given physical system is not necessarily due to a stochastic dynamics (namely to the action of a large number of excited degrees of freedom); it could be generated by the chaotic (even though deterministic) dynamics of a limited number of collective modes (see, e.g., Eckmann & Ruelle 1985). In the latter situation, the appropriate model to use is a system of a few deterministic ordinary differential equations. In the case of quasars, is not possible "a priori" to exclude that their irregular light curves could be ascribed to a situation of low-dimensional deterministic chaos, rather than to a fundamental stochastic nature of the dynamics. In our opinion, however, it is hard to think that the physical conditions of a system as complex as the central regions of a quasar could be described in terms of a small number of active modes. At the present level of knowledge, it is more reasonable to assume that the physical quantities such as the temperature, the density, the emissivity, etc., may be subject to random fluctuations due, for example, to small changes in the accretion rate of the black hole.

In any case, here we consider some of the standard methods used to search for the presence of low-dimensional deterministic chaos from a measured time series, and we show how a blind aplication of these methods may lead to erroneous conclusions in the absence of a clear information on the physics of the system (see also Osborne & Provenzale 1989; Provenzale, Osborne, & Soj 1991).

### 4.1. *Definitions and Outlines*

The basic fact underlying the practical interest of deterministic chaos is the discovery that even very simple systems, described by a few coupled nonlinear ordinary differential equations, can have solutions as unpredictable as a coin toss (Lorenz 1963; see Eckman & Ruelle 1985 for a review). The idea thus grew that the complex and irregular behavior of some physical systems could be due to the presence of deterministic chaos in the system phase space and not necessarily to a stochastic nature of the system dynamics. A large number of carefully controlled laboratory experiments have now been conducted in order to determine the role of deterministic chaos in the dynamics of irregular systems; in many cases a clear evidence of the presence of low-dimensional deterministic chaos in the system phase-space has been obtained (Brandstater et al. 1983; Malraison et al. 1983; Ciliberto & Gollub 1984, 1985; Swinney & Gollub 1986). Similar approaches have been considered also in the analysis of the variability of astronomical objects (e.g., Goupil, Auvergne, & Baglin 1988; Lochner, Swank, & Szymkowiak 1989; Cannizzo, Goodings, & Mattei 1990; Kollath 1990; Harding, Shinbrot, & Cordes 1990). In the majority of cases, the low-dimensional chaotic dynamics plays a dominant role only in the transition from a regular flow (e.g., a laminar flow in a fluid dynamical context) to fully developed turbulent conditions. Another common case is represented by systems in which there is a competition among a small number of oscillatory modes; in this case the system may chaotically wander from one oscillatory state to another. In general, low-dimensional chaos is associated with a limited *space complexity* of the system, i.e., with the existence of long space correlations. It is still unclear whether chaotic dynamics may play a relevant role in fully developed conditions.

For driven and damped systems (the most frequent in nature), a common origin of low-dimensional chaos is related to the presence of a *strange attractor* in the system phase space (Guckheneimer & Holmes 1983; Lichtenberg & Lieberman 1983; Eckmann & Ruelle 1985). In general, strange attractors have fractal properties, characterized by a *fractal dimension D* which is larger than their topological dimension $D_T = 1$ (since a strange attractor is a curve from a topological point of view). In general, the larger the dimension of the strange attractor, the more chaotic is the dynamics of the system. A way of quantitatively characterizing the degree of chaoticity is in terms of the sign of the largest *Liapunov exponent* of the dynamics: a positive Liapunov exponent corresponds to a chaotic dynamics with sensitive dependence on initial conditions and exponential divergence of nearby phase space orbits. In this case, even an infinitesimal error on the initial conditions is rapidly amplified; the state of the system thus becomes unpredictable.

### 4.2. *Methods*

The attractor dimension is an important physical quantity since it is related to the number of excited modes in the system.

In general, if a driven and damped *deterministic* system is dominated by the presence of an attractor with dimension $D$, then an estimate of the number $n$ of modes necessary to describe the system evolution is given by $n = 2D + 1$, i.e., the system dynamics could be in principle modeled by $n$ coupled nonlinear ordinary differential equations (Mané 1981). This result has been rigorously proven for nonfractal attractors; traditionally, it is believed to hold also for fractal ones. The above observations have stimulated the development of methods for reconstructing the system phase space and for calculating the fractal dimension of the possibly existing strange attractor from a measured time series (Takens 1980; Packard et al. 1980). Given a (scalar) time series $x(t_i)$, $i = 1, \ldots, N$, a common method to obtain a pseudo–phase space of the system is to consider the $d$-dimensional vector $\boldsymbol{x}(t_i)$ built by the scalar signal itself and by the $(q - 1)$ time-delayed values

$$\boldsymbol{x}(t_i) = \{x(t_i), x(t_i - \tau), x(t_i - 2\tau), \ldots, x[t_i - (d - 1)\tau]\} ,$$

where $\tau$ is an appropriate time delay which may be fixed by several methods; see, e.g., Fraser & Swinney (1986). Clearly, the results must be independent on $\tau$. The time-embedding procedure may be physically understood as a substitution of the actual phase space variables with the "numerical" time derivatives of the signal. The next step is then to study the properties of the system in the pseudo–phase spaces at increasing values of the *embedding dimension d*. To this end, a particularly useful method has proven to be the calculation of the correlation integral (Grassberger & Procaccia 1983a, b) given by

$$C_d(r) = \frac{1}{N^2} \sum_{i,j=1}^{N} \Theta[r - |\boldsymbol{x}(t_i) - \boldsymbol{x}(t_j)|] ,$$

where $\Theta$ is the Heaviside step function; the correlation integral $C_d(r)$ measures the probability that two points of the time series in the reconstructed (pseudo)–phase space with dimension $d$ are closer than the distance $r$. If the system dynamics is governed by a strange attractor, it is possible to show that at small $r$

$$C_d(r) \propto r^{D_2(d)}$$

and that

$$\lim_{d \to \infty} D_2(d) = D_2 ,$$

where $D_2$ is the correlation dimension of the strange attractor; $D_2$ is an approximation to the fractal dimension of the attractor. Another useful quantity which can be extracted from the correlation integral is the $K_2$ entropy defined as (Grassberger & Procaccia 1983b)

$$K_2 = \lim_{d \to \infty} K_2(d) ,$$

where

$$K_2(d) = \frac{1}{\tau} \log \frac{C_d(r)}{C_{d+1}(r)} .$$

The $K_2$ entropy is an approximation to the Kolmogorov-Sinai invariant entropy $K$. This latter is a measure of the degree of chaoticity of a system: regular systems are characterized by a null entropy, whereas chaotic and stochastic systems are characterized by a finite and, respectively, divergent (i.e., continuously growing) value of $K$. The $K$ entropy is related to the Liapunov exponents of the dynamics; in particular, it is an upper bound to the sum of the positive Liapunov exponents (see, e.g., Eckmann & Ruelle 1985). The quantity $1/K$ has an important physical meaning since it provides an estimate of the *predictability time* of the system.

The convergence of the correlation dimension at increasing $d$'s, and the finite value of the $K_2$ entropy, are rigorous results for systems which are dominated by a low-dimensional strange attractor. However, in the analysis of experimental signals this route has been reversed, and the phase space reconstruction methods, the calculation of the correlation dimension and of the $K_2$ entropy have been used on systems whose detailed dynamics is unknown. In this approach, the phase-space reconstruction is pursued on a given experimental signal and a family of pseudo–phase spaces with increasing embedding dimension $d$ is generated. In each of these spaces, the correlation integral is computed, and the scaling properties of $C_d(r)$ are analyzed. When the correlation integral has a power-law behavior, then the exponent $D_2(d)$ is computed. If, for increasing values of $d$, the scaling exponent $D_2(d)$ saturates to a finite value $D_2$, the system dynamics is supposed to be governed by a strange attractor with correlation dimension $D_2$. The $K_2$ entropy is computed as well, a finite value of $K_2$ is considered as a further indication of the presence of a strange attractor in the system phase space. Thus, finite and convergent values of the dimension $D_2$ and of the $K_2$ entropy have been taken almost as *proofs* of the presence of low-dimensional chaos in the dynamics of systems with irregular behavior.

The above picture, however, may be misleading, since there are simple stochastic processes, characterized by power-law power spectra, which lead to a finite value of the estimated correlation dimension $D_2$ and to a converging estimate of the $K_2$ entropy when a time-embedding procedure is applied (Osborne & Provenzale 1989; Provenzale, Osborne, & Soj 1991). Here we consider the two signals reported in Figures 2*a* and 2*b*, and we show that in this case an analogous situation is found as well. Figure 11 shows the exponent $D_2(d)$ versus the embedding dimension $d$ as computed from the time series produced by the linear stochastic system (Fig. 2*a*) and by the nonlinear one (Fig. 2*b*). No significant difference is observed between the two cases; for both systems the dimension esti-

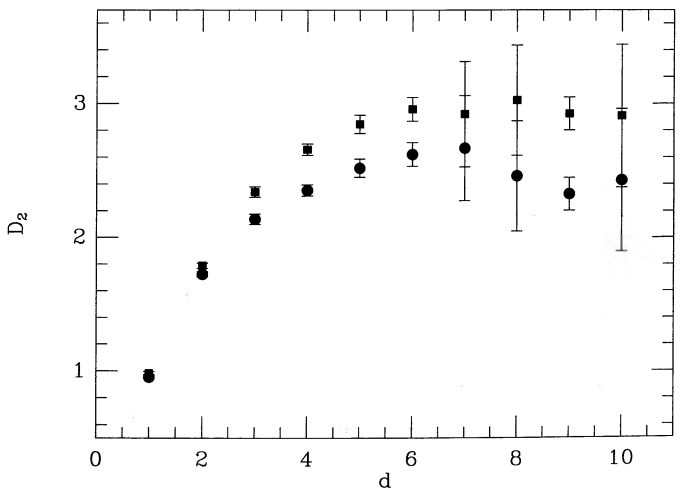


FIG. 11.—Correlation dimension $D_2(d)$ vs. the embedding dimension $d$ for the time series shown in Fig. 2*a* (*filled squares*) and in Fig. 2*b* (*filled circles*). The error bars are the 95% confidence limits on the linear least-squares fit of $\log C_d(r)$ vs. $\log (r)$.

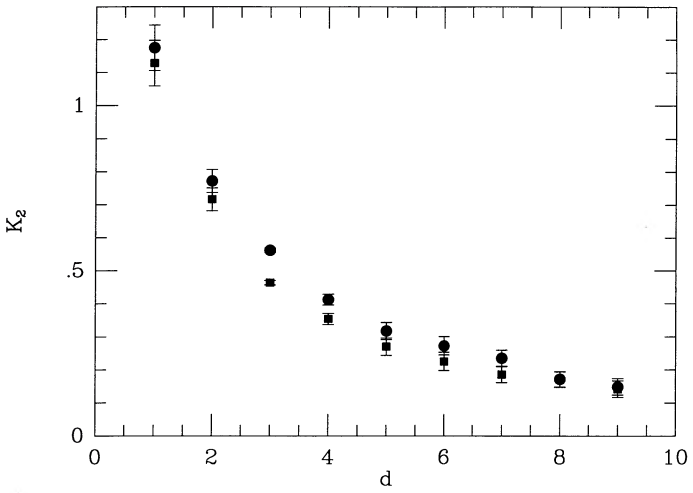


FIG. 12.—Correlation entropy $K_2(d)$ vs. $d$ for the time series shown in Fig. 2*a* (*filled squares*) and in Fig. 2*b* (*filled circles*). The error bars are the standard deviations on log $[C(n)/C(n+1)]$ in the scaling range.

mate converges to a value which is fixed by the logarithmic slope of the power spectrum of the signals, independent of the differences in the phase distribution. Since the power spectrum is approximately the same, the saturation dimension is the same for the two signals. Analogously, the estimated $K_2$ entropy converges for both signals, as shown by Figure 12. Thus, not only the dimension and entropy estimates (through a time-embedding procedure) would erroneously suggest the presence of deterministic chaos (a fact which is absurd since the two signals have been produced by stochastic processes), but they are also unable to distinguish between the two time series. Once more, it is necessary to have some clear knowledge on the system dynamics before drawing any conclusion. In other words, extreme care must be taken before claiming the presence of chaos on the basis of the analysis of just one or a few time series. Finally, as an example we show in Figure 13 the correlation dimension $D_2(d)$ versus the embedding dimension $d$ for the (X-ray) light curve of the BL Lac object PKS 2155−304: no saturation is present in the dimensions, so that a stochastic nature is strongly suggested for this signal.

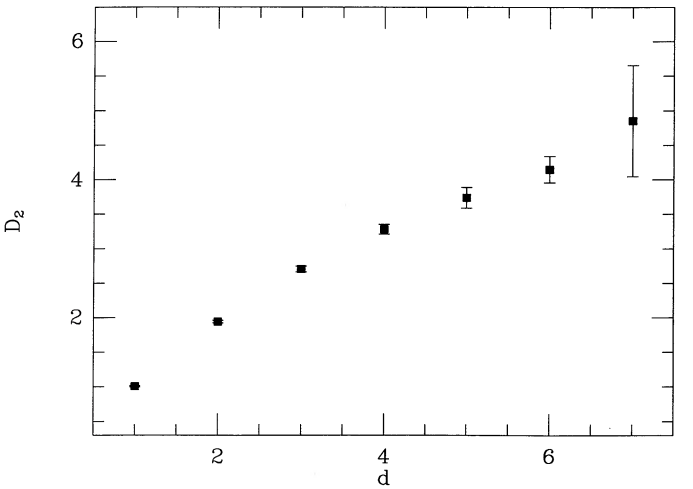


FIG. 13.—Correlation dimension $D_2(d)$ vs. $d$ for the (X-ray) light curve of the BL Lac PKS 2155−304. The error bars are the 95% confidence limits on the linear least-squares fit of log $C_d(r)$ vs. log $(r)$.

## 5. COMPOSITE STOCHASTIC SYSTEMS

The previous section has been developed with the implicit assumption that the dynamics of physical process under study is due to the evolution of a single system. In the case of quasars, this means that the variations of the flux emitted are due to the evolution of a single component (e.g., the inner part of an accretion disk or the lensing of the light through an intervening galaxy). However, other scenarios are a priori possible. For example, the dynamics of the process could be due to the evolution of several independent systems (in this case little information can be retrieved by the simple analysis of a time series), or to the evolution of a system composed by many subunits. In the latter case, if the behavior of any subunit is independent on the dynamics of the other ones, the observed time series can be thought to be the realization of a shot noise process. In past years, various methods for deriving the shape of the "shots" from an observed time series have been proposed (Fahlman & Ulrych 1975, 1976; Scargle 1981, 1990). These methods are generally based on a fit with a linear MA (moving–average) model of the data (the MA model is closely related to the shot noise process; see, e.g., Scargle 1981). However, before using these methods it is necessary to check the linearity of the time series (in other words it is necessary to check the "independency" of the bursts). In fact, if the time series is stationary but nonlinear (namely, if the bursts interact among them somewhow), then Wold's theorem (Wei 1990) assures the existence of a *linear* MA representation of the proces that, however, *has no physical meaning.*

Even more than in the situation described in the previous sections, in the case of a nonlinear, multiple subunit model, it is difficult to investigate the system dynamics in the absence of an a priori physical input. In order to elucidate this point, we have simulated a simplified version of the "hot spots" accretion disk models of Wiita et al. (1990) and Abramowicz et al. (1989). According to these authors, the variations of the quasar luminosity are due to the Poissonian formation of bright, noninteracting regions (hot spots) on the surface of an accretion disk orbiting a black hole. Contrary to what is experimentally observed (e.g., Remillard et al. 1991), the time series obtainable by these models appear uniform (see, for example, Fig. 2 of Abramowicz et al. 1989): they are not able to produce sudden bursts of large amplitude. We have simulated a nonrotating "square" accretion disk, composed by 10,000 subunits, with a uniform brightness of value 1. On the accretion disk the "hot spots" are formed according to the following rules:

1. The time occurrence of the "hot spots" follows a Poissonian statistics.
2. Every "hot spot," when it appears, completely occupies a subunit whose luminosity goes to 2.
3. The life time is equal for all the "hot spots," with an abrupt turn-on and turn-off. When a "hot spot" is overlapped by another one, its life starts from the beginning again.
4. When $n$ "hot spots" occupy the same area, the luminosity of the subunit increases to $2^n$. This kind of multiplicative nonlinearity has been chosen following the results obtained by Vio et al. (1991).

Figure 14*a* shows a typical light curve (1000 time units long) generated by this model. Figure 14*b* shows the corresponding light curve without the nonlinear mechanism (in other words in the second case, when $n$ "hot spots" occupy the same area, the luminosity of the subunit becomes $n \times 2$). From the com-

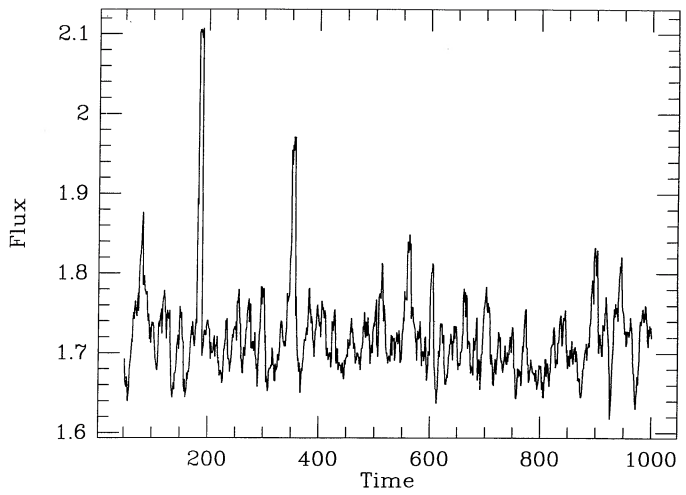


FIG. 14*a*

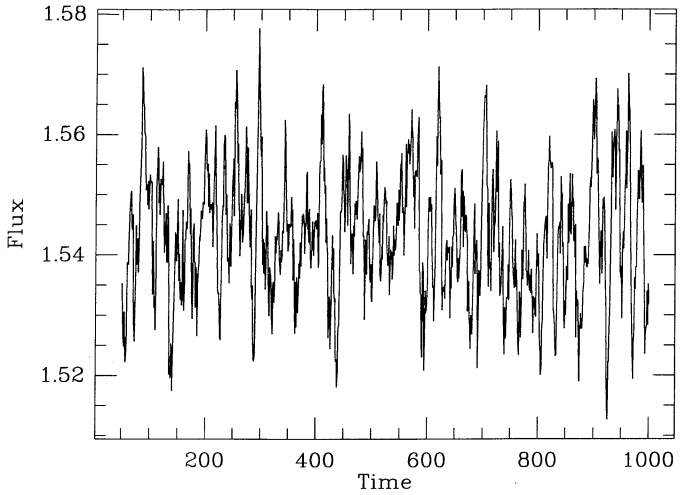


FIG. 14*b*

FIG. 14.—Time series generated by the disk model described in the text. (*a*) Nonlinear model (the number of bursts for time units = 50, life of the bursts = 70 time units, frequency of the signal sampling = 10 time units, 1000 points in the time series, brightening factor = 2). (*b*) Corresponding linear model (see text).

parison of the two figures, it is clear that only the nonlinear model is able to produce bursts. However, the Keenan test (95% confidence) is unable to realize the nonlinearity of this time series. The problem is that "in se" the process is not entirely nonlinear: the nonlinear component is due only to the overlapping "hot spots," while the contribution of the isolated "hot spots" can be regarded as a shot noise (and therefore linear) process. Without physical information, the two contributions cannot be separated, and therefore the process cannot be identified.

## 6. CONCLUSIONS

In this paper we have examined some of the possible statistical approaches to the analysis of time series in astronomy. The results which we have obtained can be summarized as follows:

1. The classical statistical methods (e.g., PS, SF, and covariance analysis) for the analysis of temporal data are often useless and even misleading since, unless the physical processes under study are linear, they are not able to use all the information contained in the data.

2. It is necessary to develop techniques better suited to deal with nonlinear continuous time series, since it is probable that many astrophysical signals, e.g., the light curves of quasars (Vio et al. 1991), fall into this category. The bispectrum analysis (Subba Rao & Gabr 1984; Chrysostomos & Mysore 1987), or the multifractal analysis (Mandelbrot 1982; Paladin & Vulpiani 1987; Sreenivasan & Meneveau 1988) represent a progress in this direction. In general, the procedure of randomizing the DFT phases of the signal turns out to be a powerful test for distinguishing between linear and nonlinear stochastic signals. The development of state-dependent models (Priestley 1980, 1988) is another possible approach. Most of the existing methods in the latter context, however, have been developed in the assumption of discrete systems and therefore, although useful for a statistical characterization of the processes, have a limited physical meaning.

3. The application of methods derived from the theory of dynamical systems (namely phase-space reconstruction and the use of dimension and entropy estimators), although extremely simple and fashionable, may lead to conceptual errors if a careful evaluation of the system dynamics is not pursued.

4. Especially in a nonlinear context, the derivation of the dynamics of a system from the simple analysis of an observed time series turns out to be a quite difficult task. Consequently, before attempting a physical interpretation of a given signal, it is necessary to have some a priori information on the system under study.

It is a pleasure to thank C. Barbieri for helpful discussions and suggestions; P. Andreani, L. Danese, G. De Zotti and L. Tosatto for carefully reading the manuscript; and J. Lehar for the code of the CLEAN algorithm.

## APPENDIX

## STOCHASTIC DIFFERENTIAL EQUATIONS

The most general *state space representation* of a *deterministic* linear dynamic system of order $n$ can be written in the form:

$$\dot{\boldsymbol{x}}(t) = \boldsymbol{F}(t)\boldsymbol{x}(t) + \boldsymbol{B}(t)\boldsymbol{u}(t)\,, \tag{A1}$$

where $\boldsymbol{x}(t)$ is an $n$-dimensional state vector (the $n$ dimensions corresponding to the fact that the system is described by $n$th order dynamics); $\boldsymbol{F}(t)$ is the corresponding time-dependent $n$-by-$n$ *state* matrix; $\boldsymbol{u}(t)$ is an $r$-dimensional input vector giving the system *input*; and $\boldsymbol{B}(t)$ is the corresponding $n$-by-$r$ *input* matrix. For example, the *state space representation* of the time-invariant, second-order, single-input system

$$\ddot{x}(t) + a_1\dot{x}(t) + a_2 x(t) = u(t)$$

is

$$\boldsymbol{F} = \begin{pmatrix} 0 & 1 \\ -a_2 & -a_1 \end{pmatrix}$$

$$\boldsymbol{B} = \begin{pmatrix} 0 \\ 1 \end{pmatrix}.$$

The solution of equation (A1) with initial condition $\boldsymbol{x}(t_0) = \boldsymbol{x}_0$ is (Maybeck 1979)

$$\boldsymbol{x}(t) = \boldsymbol{\Phi}(t, t_0)\boldsymbol{x}_0 + \int_{t_0}^{t} \boldsymbol{\Phi}(t, \tau)\boldsymbol{B}(\tau)\boldsymbol{u}(\tau)d\tau \,, \tag{A2}$$

where $\boldsymbol{\Phi}(\cdot, \,)$ is the *state transition matrix* defined as the $n$-by-$n$ matrix that satisfies the differential equation and initial condition:

$$d[\boldsymbol{\Phi}(t, t_0)]/dt = \boldsymbol{F}(t)\boldsymbol{\Phi}(t, t_0)$$

$$\boldsymbol{\Phi}(t_0, t_0) = \boldsymbol{I}$$

where $\boldsymbol{I}$ is the identity matrix of order $n$-by-$n$. If a dynamical system is "disturbed" by a continuous Gaussian white noise process, a natural extension of equation (A1) is

$$\dot{\boldsymbol{x}}(t) = \boldsymbol{F}(t)\boldsymbol{x}(t) + \boldsymbol{B}(t)\boldsymbol{u}(t) + \boldsymbol{G}(t)\boldsymbol{w}(t) \,, \tag{A3}$$

where $\boldsymbol{w}(t)$ is the $s$-dimensional input white noise process and $\boldsymbol{G}(t)$ is an $n$-by-$a$ matrix. The solution of equation (A3) can be *formally* written as

$$\boldsymbol{x}(t) = \boldsymbol{\Phi}(t, t_0)\boldsymbol{x}_0 + \int_{t_0}^{t} \boldsymbol{\Phi}(t, \tau)\boldsymbol{B}(\tau)\boldsymbol{u}(\tau)d\tau + \int_{t_0}^{t} \boldsymbol{\Phi}(t, \tau)\boldsymbol{G}(\tau)\boldsymbol{w}(\tau)d\tau \,; \tag{A4}$$

however, the last term in this equation cannot be evaluated properly, and thus equation (A4) has no real meaning. In fact, if we want to extend to the continuous case $\boldsymbol{w}(t)$, then it is implied that no correlation exists between $\boldsymbol{w}(t_i)$ and $\boldsymbol{w}(t_j)$, even for $t_i$ and $t_j$ separated by only an infinitesimal amount. This is contrary to the behavior exhibited by any process observed in nature. Moreover the power spectrum of such a process would be constant over *all* frequencies; that is, it would be an infinite power process: it cannot exist. It can be demonstrated (e.g., Maybeck 1979) that the correct solution of equation (A3) is given by

$$\boldsymbol{x}(t) = \boldsymbol{\Phi}(t, t_0)\boldsymbol{x}_0 + \int_{t_0}^{t} \boldsymbol{\Phi}(t, \tau)\boldsymbol{B}(\tau)\boldsymbol{u}(\tau)d\tau + \int_{t_0}^{t} \boldsymbol{\Phi}(t, \tau)\boldsymbol{G}(\tau)d\boldsymbol{\beta}(\tau) \,, \tag{A5}$$

where $\boldsymbol{\beta}(t)$ is a multivariate *Brownian motion process* of strength $\boldsymbol{Q}(t)$. This process has the following properties:

1. It is a process with independent increments, namely if $t_0 < t_1 < t_2 \cdots < t_N$ is a time partition of temporal interval $T$, and

$$\boldsymbol{\Delta}_1 = [\boldsymbol{\beta}(t_1) - \boldsymbol{\beta}(t_0)]$$

$$\boldsymbol{\Delta}_2 = [\boldsymbol{\beta}(t_2) - \boldsymbol{\beta}(t_1)]$$

$$\vdots$$

$$\boldsymbol{\Delta}_N = [\boldsymbol{\beta}(t_N) - \boldsymbol{\beta}(t_{N-1})]$$

then the increments $\boldsymbol{\Delta}_i$ are mutually independent for *any* such partition of $T$.

2. The increments are Gaussian random variables such that, for $t_1$ and $t_2$ ($t_1 < t_2$) any time instants in $T$,

$$E[\boldsymbol{\beta}(t_2) - \boldsymbol{\beta}(t_1)] = \boldsymbol{0}$$

$$E\{[\boldsymbol{\beta}(t_2) - \boldsymbol{\beta}(t_1)][\boldsymbol{\beta}(t_2) - \boldsymbol{\beta}(t_1)]^T\} = \int_{t_1}^{t_2} \boldsymbol{Q}(t)dt \,,$$

where $\boldsymbol{Q}(t)$ is a symmetric and positive semidefinite matrix. The last term in equation (A5) is a stochastic integral of Wiener. Using the properties of this integral it is possible to demonstrate that the solution of equation (A3) at a set of (not necessarily equispaced) instants $t_1, t_2, \ldots$ is given by

$$\boldsymbol{x}(t_{i+1}) = \boldsymbol{\Phi}(t_{i+1}, t_i)\boldsymbol{x}(t_i) + \boldsymbol{u}_d(t_i) + \boldsymbol{w}_d(t_i) \,, \tag{A6}$$

where

$$\boldsymbol{u}_d(t_i) = \int_{t_i}^{t_{i+1}} \boldsymbol{\Phi}(t_{i+1}, \tau)\boldsymbol{B}(\tau)\boldsymbol{u}(\tau)d\tau \,,$$

and $\boldsymbol{w}_d(\cdot)$ is an $n$-vector-valued white Gaussian discrete-time stochastic process with the following properties:

$$E[\boldsymbol{w}_d(t_i)] = \boldsymbol{0} \tag{A7}$$

$$E[\boldsymbol{w}_d(t_i)\boldsymbol{w}_d^T(t_i)] = \boldsymbol{Q}_d(t_i) = \int_{t_i}^{t_{i+1}} \boldsymbol{\Phi}(t_{i+1}, \tau)\boldsymbol{G}(\tau)\boldsymbol{Q}(\tau)\boldsymbol{G}^T(\tau)\boldsymbol{\Phi}^T(t_{i+1}, \tau)d\tau$$

$$E[\boldsymbol{w}_d(t_i)\boldsymbol{w}_d^T(t_j)] = \boldsymbol{0} \qquad t_i \neq t_j \,.$$

In this way, with a regular sampling, the solution of the system (A3) is given by the solution of an ordinary system of difference equations.

In the nonlinear case, the dynamical system can be generally represented by

$$\dot{x}(t) = f[x(t), u(t), w(t), t] . \tag{A8}$$

However, such a model is very difficult to develop rigorously (Maybeck 1982). Therefore it is necessary to limit ourselves to less general models such as

$$dx(t) = f[x(t), u(t), t]dt + G[x(t), t]d\beta(t) . \tag{A9}$$

The equation (A9) represents the so-called Itô stochastic differential equation, but unfortunately even in this simplified form it does not exist a general method to solve it. Two possible methods to accomplish this aim are (1) a local linearization of the process (Ozaki 1985) or (2) numerical methods (McShane 1974; Maybeck 1982; Mil'sthein 1974, 1978; Sancho et al. 1982; Klauder & Petersen 1985; Hernandez 1991).

## REFERENCES


Abramowicz, M. A., Bao, G., Lanza, A., & Zhang, X. H. 1989, in 23rd ESLAB Symposium on Two Topics in X-ray Astronomy (ESPA SP-296), ed. J. Hunt & B. Battrick (Noordwijk: ESA), 2, 871
Basdevant, C., Legras, B., Sadourny, R., & Beland, M. 1981, J. Atm. Sci., 38, 2305
Barbieri, C., Vio, R., Cappellaro, E., & Turatto, M. 1990, ApJ, 359, 63
Benzi, R., Paladin, G., Parisi, G., & Vulpiani, A. 1984, J. Phys. A, 17, 3521
Benzi, R., Paladin, G., Patarnello, S., Santangelo, P., & Vulpiani, A. 1986, J. Phys. A, 19, 3771
Brandstater, A., Swift, J., Swinney, H. L., Wolf, A., Farmer, J. D., Jen, E., & Crutchfield, P. J. 1983, Phys. Rev. Lett., 51, 1442
Brown, T. M., & Christensen-Dalsgaard, J. 1990, ApJ, 349, 667
Cannizzo, J. K., Goodings, D. A., & Mattei, J. A. 1990, ApJ, 357, 235
Chrysostomos, L. N., & Mysore, R. R. 1987, Proc. IEEE, 75(7), 869
Ciliberto, S., & Gollub, J. P. 1984, Phys. Rev. Lett., 52, 922
———. 1985, J. Fluid Mech., 158, 381
Deeming, T. J. 1975, Ap&SS, 36, 137
Eckmann, J.-P., & Ruelle, D. 1985, Rev. Mod. Phys., 57, 617
Fahlman, G. G., & Ulrych, T. J. 1975, ApJ, 201, 277
———. 1976, ApJ, 209, 663
———. 1982, MNRAS, 199, 53
Fraser, A. M., & Swinney, H. L. 1986, Phys. Rev. A, 33, 1134
Frisch, U., & Parisi, G. 1985, in Turbulence and Predictability in Geophysical Fluid Dynamics and Climatology, ed. M. Ghil, R. Benzi, & G. Parisi (Amsterdam: North-Holland), 84
Goupil, M. J., Auvergne, M., & Baglin, A. 1988, A&A, 196, L16
Grassberger, P., & Procaccia, I. 1983a, Physica, D9, 189
———. 1983b, Phys. Rev. A, 28, 2591
Guckenheimer, J., & Holmes, P. 1983, Nonlinear Oscillations, Dynamical Systems and Bifurcation of Vector Fields (New York: Springer)
Halsey, T. C., Jensen, M. H., Kadanoff, L. P., Procaccia, I., & Shraiman, B. I. 1986, Phys. Rev. A, 33, 1141
Harding, A. K., Shinbrot, T., & Cordes, J. M. 1990, ApJ, 353, 588
Heck, A., Manfroid, J., & Mersch, G. 1985, A&AS, 59, 63
Heck, A., ed. 1990, Vistas Astron., 33
Heck, A., & Perdang, J. ed. 1991, Applying Fractals in Astronomy (Berlin: Springer)
Hernandez, D. B. 1991, Sistemi Dinamici Stocastici (Bologna: Pitagora)
Horne, J. H., & Baliunas, S. L. 1986, ApJ, 302, 757
Keenan, D. M. R. 1985, Biometrika, 72, 39
Klauder, J. R., & Petersen, W. P. 1985, SIAM Num. An., 22, 1153
Koen, K. 1990, ApJ, 348, 700
Kollath, Z. 1990, MNRAS, 247, 377
Lawrence, A., Watson, M. G., Pounds, K. A., & Elvis, M. 1987, Nature, 325, 694
Lichtenberg, A., Lieberman, M. 1983, Regular and Stochastic Motion (New York: Springer)
Lochner, J. C., Swank, J. H., & Szymkowiak, A. E. 1989, ApJ, 337, 823
Lorenz, E. 1963, J. Atm. Sci., 20, 130
Malraison, B., Atten, P., Berge, P., & Dubuois, M. 1983, J. Phys. (Paris), 44, L897
Mandelbrot, B. B. 1982, The Fractal Geometry of Nature (San Francisco: Freeman)
Mané R. 1981, in Lecture Notes in Mathematics, 898, Detecting Strange Attractors in Turbulence, ed. D. A. Rand & L. S. Young (Berlin: Springer), 230
Manwell, T., & Simon, M. 1968, AJ, 73, 407
Marple, S. L. 1987, Digital Spectral Analysis With Applications (Englewood Cliffs, N.J.: Prentice-Hall)
Martinez, V., Jones, B. J. T., Dominguez-Tenreiro, R., & van de Weygaert, R. 1990, ApJ, 357, 50
Maybeck, P. S. 1979, Stochastic Models, Estimation, and Control, Vol. 1 (New York: Academic)
Maybeck, P. S. 1982, Stochastic Models, Estimation, and Control, Vol. 2 (New York: Academic)
McHardy, I. M. 1989, in 23rd ESLAB Symposium on Two Topics in X-Ray Astronomy (ESA SP-296), ed. J. Hunt & B. Battrick (Noordwijk: ESA), 2, 1111
McHardy, I. M., & Czerny, B. 1987, Nature, 325, 696
McShane, E. J. 1974, Stochastic Calculus and Stochastic Models (New York: Academic)
Mil'sthein, G. N. 1974, Theor. Prob. Appl., 19, 557
———. 1978, Theor. Prob. Appl., 23, 396
Moore, R. L., et al. 1982, ApJ., 260, 415
Nemec, A. F. L., & Nemec, J. M. 1985, AJ, 90, 2317
Osborne, A. R., & Provenzale, A. 1989, Physica, D35, 357
Ozaki, T. 1985, in Handbook of Statistics, ed. E. J. Hannan & P. R. Krishnaiah (Amsterdam: North-Holland), 5, 25
Packard, N. H., Crutchfield, J. P., Farmer, J. D., & Shaw, R. S. 1980, Phys. Rev. Lett., 45, 712
Pandit, M., & Wu, S. M. 1975, Biometrika, 62, 497
Paladin, G., & Vulpiani, A. 1987, Phys. Rep., 156, 147
Pietronero, L., & Tosatti, E., ed. 1986, Fractals in Physics (Amsterdam: North-Holland)
Press, W. H., & Rybicki, G. B. 1989, ApJ, 338, 277
Priestley, M. B. 1980, J. Time Series Anal., 1, 47
———. 1988, Non-linear and Non-stationary Time Series Analysis (New York: Academic)
Provenzale, A., Osborne, A. R., & Soj, R. 1991, Physica, D47, 361
Remillard, R. A., Grossan, B., Bradt, H. V., Ohashi, T., Hayashida, K., Kakino, F., & Tanaka, Y. 1991, Nature, 350, 589
Roberts, D. H., Lehar, J., & Dreher, W. 1987, AJ, 83, 968
Sancho, J. M., San Miguel, M., Katz, S. L., & Gunton, J. D. 1982, Phys. Rev. A, 26, 1589
Scargle, D. S. 1981, ApJS, 45, 1
———. 1982, ApJ, 263, 835
———. 1989, ApJ, 343, 874
———. 1990, ApJ, 359, 469
Schertzer, D., & Lovejoy, S. 1987, J. Geophys. Res., 92, 9693
Segal, M., & Weinstein, E. 1987, Proc. IEEE, 75(5), 727
Simonetti, J. H., Cordes, J. M., & Heeschen, D. S. 1985, ApJ, 296, 46
Sreenivasan, K. R., & Meneveau, C. 1988, Phys. Rev. A, 38, 6287
Sturrock, P. A., & Shoub, E. C. 1982, ApJ, 256, 788
Subba Rao, T., & Gabr, M. M. 1984, An Introduction to Bispectral Analysis and Bilinear Time Series Models (New York: Springer)
Swingler, D. N. 1989, AJ, 97, 280
Swinney, H. L., & Gollub, J. P. 1986, Physica, 18D, 448
Tagliaferri, G., Stella, L., Maraschi, L., Treves, A., & Morini, M. 1989, in BL Lac Objects, ed. L. Maraschi, T. Maccacaro, & M. H. Ulrich (New York: Springer), 314
Takens, F. 1981, in Lecture Notes in Mathematics, 898, Detecting Strange Attractors in Turbulence, ed. D. A. Rand & L. S. Young (Berlin: Springer), 366
Terrel, J., & Olsen, K. H. 1970, ApJ, 161, 399
Tong, H. 1983, Threshold Models in Non-Linear Time Series Analysis (New York: Springer)
Ulrich, T. J., & Bishop, T. N. 1975, Rev. Geophys. Space Phys., 13, 183
Vio, R., Cristiani, S., Lessi, O., & Salvadori, L. 1991, ApJ, 380, 351
Wei, W. W. S. 1990, Time Series Analysis (New York: Addison-Wesley)
Witta, P. J., Miller, H. R., Carini, M. T., & Rosen, A. 1991, in IAU Colloq. 129, Structure and Emission Properties of Accretion Disks, ed. C. Bertout, S. Collin-Souffrin, J. P. Lasota, & J. Tran Than Van (Paris: Editions Frontières), 557